

# 1 **Viability of greenhouse gas removal via the artificial addition of volcanic** 2 **ash to the ocean**

3 Jack Longmana,<sup>b,c\*</sup> Martin R. Palmer<sup>b</sup>, Thomas M. Gernon<sup>b</sup>

4 <sup>a</sup> Marine Isotope Geochemistry, Institute for Chemistry and Biology of the Marine  
5 Environment (ICBM), University of Oldenburg, PO Box 2503, 26111 Oldenburg, Germany

6 <sup>b</sup> School of Ocean and Earth Sciences, University of Southampton, Southampton SO14 3ZH,  
7 UK

8 <sup>c</sup> School of Geography and the Environment, University of Oxford, South Parks Road,  
9 Oxford, OX1 3QY, UK

10 \*Corresponding Author: jack.longman@uni-oldenburg.de

## 11 **Abstract**

12 Attempts to mitigate human contributions to climate change have become a highly debated  
13 topic, as it becomes evident that optional global emission reductions are not being adhered to  
14 by many nations. Therefore, substantial research is taking place into negative carbon  
15 technologies that actively reduce the amount of atmospheric carbon dioxide (CO<sub>2</sub>), via  
16 greenhouse gas removal (GGR). Various GGR methods have been proposed, from reforestation  
17 to ocean fertilisation. Here, we discuss the advantages of an approach based on the enhanced  
18 input of tephra to the ocean, to increase the drawdown of atmospheric CO<sub>2</sub>. Natural addition  
19 of tephra to the ocean results in enhanced organic matter preservation in sediment; hence  
20 augmenting its delivery should raise the level of sequestration. Our calculations indicate  
21 offshore tephra addition could sequester 2750 tonnes of CO<sub>2</sub> per 50,000 tonnes of ash delivered  
22 (a typical bulk carrier's capacity). The cost is estimated to be ~\$55 per tonne of CO<sub>2</sub>  
23 sequestered and is an order of magnitude cheaper than many other proposed GGR technologies.  
24 Further advantages include; tephra addition is simply an augmentation of a natural Earth  
25 process, it is a low technology approach that requires few developments, and it may sequester  
26 carbon for thousands of years. Hence, we suggest offshore tephra addition warrants further  
27 investigation to assess its viability.

## 28 **Keywords**

29 Greenhouse Gas Removal, geoengineering, offshore tephra addition, volcanic ash, diagenesis,  
30 climate change

### 31 **Introduction**

32 Proposals have recently been made to remediate human contributions to climate change  
33 through geoengineering, leading to considerable discussion of the topic (Royal Society, 2018).  
34 To ensure the world stays below the IPCC upper limit to “safe” warming (IPCC, 2018),  
35 additional measures other than non-binding agreements will be required (Haszeldine et al.,  
36 2018; Tollefson, 2018). Hence, Greenhouse Gas Removal (GGR), via geoengineering, has  
37 been posited to reduce levels of anthropogenic carbon dioxide (CO<sub>2</sub>) in the atmosphere, thus  
38 avoiding large-scale impacts of climate change such as ecosystem collapse and major changes  
39 in ocean circulation (Lomax et al., 2015; Steffen et al., 2018).

40 A variety of GGR methods have been proposed, from reforestation and habitat restoration (e.g.  
41 (e.g. Bastin et al., 2019), to infrastructural changes, such as low-carbon concrete production  
42 (Ghouleh et al., 2017) and the use of biomass in building materials (e.g. Ramage et al., 2016).  
43 Other GGR proposals involve enhancing the rate at which the Earth’s natural carbon cycle  
44 sequesters atmospheric CO<sub>2</sub> in natural sinks (Royal Society, 2018). Examples of natural cycle  
45 manipulation include increasing the alkalinity of the ocean (i.e., reversing ocean acidification  
46 (Renforth and Henderson, 2017)), enhancing mineral carbonation (i.e., converting silicate  
47 rocks into carbonates (Matter et al., 2016)) and ocean fertilization (i.e., enhancing  
48 photosynthetic carbon removal (Boyd et al., 2007)).

49 All proposed GGR interventions have associated risks, and face scientific, economic and  
50 societal barriers to implementation. For example, repurposing terrestrial biomass for carbon  
51 sequestration necessarily requires the utilization of agricultural land currently used to produce  
52 food. Manipulation of natural cycles also suffer from an unpalatable image due to perceived  
53 meddling with the natural world, and potential impacts on ecosystems (Royal Society, 2018).

54 No single mechanism of emissions reduction or GGR can feasibly halt the rise in atmospheric  
55 CO<sub>2</sub> levels (Royal Society, 2018), so it is beneficial to consider a range of emissions reduction  
56 and GGR strategies that have lesser risks and implementation barriers, rather than adoption of  
57 a single big impact, high-risk strategy. Hence, we present a potential GGR mechanism based  
58 on enhanced input of the products of explosive volcanism (Figure 1) into the oceans. This  
59 approach builds on the role that natural tephra deposition in the oceans plays in the carbon  
60 cycle (Figure 2) (Longman et al., 2019) and examines the potential enhancement of these  
61 natural processes to achieve GGR. Based on real-world data, we calculate the potential of the  
62 proposed method to sequester atmospheric carbon, and provide an estimate of likely costs.

### 63 **The Approach**

64 It is estimated that the global amount of organic carbon (C<sub>org</sub>) reaching the seafloor is  
65 equivalent to 8.4 Gt CO<sub>2</sub> a<sup>-1</sup>, of which ~13% is buried and 87% returned to the ocean-  
66 atmosphere (Burdige, 2007). The variety of processes controlling the C<sub>org</sub> burial efficiency  
67 (CBE) lead to wide geographical variations in this value, from >70% to <0.3%; (Dunne et al.,  
68 2007). Within these processes there are four distinct mechanisms by which tephra deposition  
69 enhances CBE (Longman et al., 2019), outlined below.

#### 70 *Fertilization*

71 Tephra releases nutrients, such as dissolved Iron (Fe), to surface waters when it falls into the  
72 oceans, and may thus stimulate biological productivity where availability of nutrients limits  
73 phytoplankton growth (Olgun et al., 2011). This process has been the subject of extensive study  
74 (e.g., see Olgun et al. (2011) and Duggen et al. (2010) for reviews). For example,  
75 phytoplankton blooms occurred when tephra was deposited in the nutrient-poor NE Pacific  
76 Ocean following eruption of Kasatochi volcano (Langmann et al., 2010; Olgun et al., 2011), in  
77 the vicinity of the Mariana Islands following the 2003 Anatahan eruption (Lin et al., 2011),  
78 after the eruption of Miyake-jima in 2000 (Uematsu et al., 2004), and potentially in the

79 Southern Pacific after the eruption of Pinatubo in 1991 (Siegenthaler and Sarmiento, 1993).  
80 Other research suggests subduction zone-related ash deposition may play a role in controlling  
81 productivity (Duggen et al., 2007). In each case, the increased productivity sequestered CO<sub>2</sub>  
82 from the ocean-atmosphere. For example, the 2008 eruption of Kasatochi led to the export of  
83 ~0.01 Pg carbon from the upper ocean (Hamme et al., 2010). Carbon was removed from the  
84 upper oceans when phytoplankton (and their consumers) settled out of the upper ocean and into  
85 the deep ocean (the ‘biological pump’; Sarmiento and Gruber, 2006). In addition to accelerating  
86 the rate of the biological pump (Fig. 2), tephra deposition in the surface oceans also likely  
87 enhances the transport of organic carbon (C<sub>org</sub>) from surface oceans into deeper water because  
88 plankton debris may become physically associated with the negatively buoyant particles (e.g.,  
89 Rubin et al., 2011). This leads to the incorporation of dense, Fe-rich dust (and by analogy  
90 tephra) in algal colonies, ballasting the tephra and enhancing sinking rates (Pabortsava et al.,  
91 2017).

#### 92 *Dissolved Oxygen (O<sub>2</sub>) consumption*

93 Much of the Fe contained within tephra is in the form of Fe<sup>II</sup> (Maters et al., 2017), which is  
94 highly reactive and rapidly oxidized to Fe<sup>III</sup> through pore water O<sub>2</sub> consumption. This process  
95 also occurs during tephra transport through the water column, but due to ballasting tephra  
96 settling rates are too fast for this to be significant, leading to the export of a large proportion of  
97 Fe<sup>II</sup> to the sediment (Hembury et al., 2012). Once sufficient tephra (i.e., a layer >0.5 cm thick)  
98 accumulates on the ocean floor, oxidation of Fe<sup>II</sup> in the tephra causes dissolved O<sub>2</sub>  
99 concentrations fall to zero within sediment pore waters, reducing the exposure of the newly  
100 deposited C<sub>org</sub> to oxidative processes (Haeckel et al., 2001; Hembury et al., 2012). Because  
101 the oxidation of labile C<sub>org</sub> in marine sediments is critically dependent on dissolved O<sub>2</sub> levels  
102 in pore water (Hartnett et al., 1998), the presence of tephra likely enhances C<sub>org</sub> preservation in  
103 sediments and further sequesters CO<sub>2</sub> from the ocean-atmosphere system (Fig. 2).

104        *Colloidal association*

105 Tephra contains high concentrations of reactive Fe Mn and Al (Homoky et al., 2011). These  
106 reactive phases form stable colloids with C<sub>org</sub> (Lalonde et al., 2012), inhibiting C<sub>org</sub> oxidation  
107 and enhancing preservation (Fig. 2). Notably, the colloid–C<sub>org</sub> complexes are sufficiently stable  
108 to protect C<sub>org</sub> from oxidation even if they are transported from shelf environments to the deep  
109 sea (Dunne et al., 2007).

110        *Authigenic carbonate formation*

111 Tephra is also rich in divalent cations released into sediment pore waters during diagenesis  
112 (Gieskes, 1983; Murray et al., 2018). One proposed method of GGR is to increase ocean  
113 alkalinity, through artificial addition of divalent cations to the ocean (Kheshgi, 1995; Renforth  
114 and Henderson, 2017). Within marine sediments, cations released from tephra react with the  
115 enhanced alkalinity created by C<sub>org</sub> oxidation, resulting in the precipitation of authigenic  
116 calcium carbonate and calcium-magnesium carbonate (Ca(Mg)CO<sub>3</sub>). Again, this process  
117 effectively locks carbon derived from C<sub>org</sub> into a form that may be stable for millennia (Schrag  
118 et al., 2013).

119        **Technology readiness**

120 Addition of tephra to the oceans requires no new technology and ocean fertilization  
121 experiments have proven feasible (Boyd et al., 2007). In mesoscale experiments, artificial Fe  
122 addition enhances phytoplankton productivity in high nutrient, low chlorophyll environments  
123 by alleviating Fe-related nutrient limitation (Martin and Fitzwater, 1988). Phytoplankton  
124 blooms as a result of natural tephra addition to HNLC regions have also been observed,  
125 confirming the fertilizing potential of tephra in these environments (Langmann et al., 2010;  
126 Olgun et al., 2011). The mechanisms relating to the impact of tephra within seafloor sediments  
127 indicate that sequestration of plankton-produced C<sub>org</sub> may occur over millennial timescales, but

128 an assessment of the amount of tephra deposition required to enable significant levels of carbon  
129 sequestration is required.

130 Most active terrestrial volcanoes produce tephra and, with the exception of Australia, it is  
131 produced on every continent (Fig. 3). Tephra is one of the most common components of global  
132 oceanic sediments, such that it comprises ~25% of Pacific Ocean sediments (Scudder et al.,  
133 2016), and with an estimated yearly flux of ash to the Pacific Ocean of  $0.13 - 0.22 \times 10^{15} \text{ g a}^{-1}$   
134 (Olgun et al., 2011). Quarrying of recent tephra (optimal for this proposed method) provides  
135 aggregate for cement works and road surfaces, but supplies are not limiting. Large recent  
136 deposits of basaltic tephra are located across the globe (Fig. 3). In addition, bentonite clay  
137 (diagenetically altered tephra) mining is well-established (Eisenhour and Brown, 2009), so  
138 novel, energy-intensive, extraction techniques are not required. Most tephra extraction occurs  
139 in open pits using bucket loaders so would only require sorting of the unconsolidated tephra to  
140 grain size  $<63\mu\text{m}$ , the fraction containing most Fe-rich minerals (Homoky et al., 2011).

#### 141 **Storage potential and longevity of storage**

142 The gross storage potential is defined here as the increase in CO<sub>2</sub> storage resulting from tephra  
143 addition to the oceans. The net storage potential is the gross storage minus the CO<sub>2</sub> requirement  
144 of delivering the tephra to the oceans; although the latter value is not included in most methods  
145 evaluated in the GGR Royal Society report (Royal Society, 2018).

146 Here, we provide an estimate of the potential carbon storage using the Peru margin as an  
147 example due to its naturally high primary productivity, resulting from upwelling of nutrient-  
148 rich Pacific bottom waters (Pennington et al., 2006). The high productivity leads to depletion  
149 of O<sub>2</sub> in the water column, and an oxygen minimum zone (OMZ) bathing sediment to depths  
150 of 400m (Bohlen et al., 2011). As a result, the sediments contain up to 15% C<sub>org</sub> below the  
151 OMZ (Arthur et al., 1998). CBE increases from 18% on the inner shelf (with no OMZ) to  
152 average of 47% below the OMZ (Dale et al., 2015) due to the reduced oxidant exposure.

153 **Table 1** contains an estimate of the key parameters required to assess gross and net potential  
154 storage of  $C_{org}$  on the inner shelf through the addition of tephra to these sediments. In these  
155 calculations, we assume that reduced oxidant exposure in the sediments resulting from tephra  
156 addition, yields a similar increase in CBE to that resulting from the OMZ. As with all GGR  
157 strategies, there are large uncertainties in evaluating these parameters, in particular CBEs.  
158 Nevertheless, this exercise is useful for provide a comparison with other GGR strategies with  
159 similar uncertainties ([Royal Society, 2018](#)) (**Table 2**).

160 The calculated net potential removal is ~2300 t of  $CO_2$  per 50,000 t of tephra delivered to the  
161 oceans per year. The impact of Fe fertilization has a limited duration, but each addition of  
162 tephra to the seafloor will impact  $C_{org}$  storage for hundreds to thousands of years. **Table 1**  
163 assumes a tephra layer of 5 mm is required to achieve the calculated increase in CBE, but  
164 microelectrode studies of tephra deposited on the seafloor reveal that pore water dissolved  $O_2$   
165 concentrations can fall to <50% of bottom water levels within 1 mm of the sediment-water  
166 interface ([Hembury et al., 2012](#)). Thus, the dependence of CBE on dissolved  $O_2$  exposure  
167 times ([Hartnett et al., 1998](#)) would likely lead to enhanced  $CO_2$  storage even under minimal  
168 tephra loading. Note also, that the natural CBEs observed on the Peru margin are not typical  
169 of shelf sediments. The average CBE in sandy sediments, that represent 70% of the global  
170 area of continental shelves with water depths <200 m, is ~1% ([Burdige, 2007](#)). Hence,  
171 selection of optimal seafloor sites for large increases in gross potential storage (i.e. large  $C_{org}$   
172 fluxes, but low CBE, delivery of optimum amounts of tephra to achieve maximum increase in  
173  $C_{org}$  preservation) and net potential storage (i.e. close to readily accessible tephra deposits) may  
174 yield potential  $CO_2$  storage rates similar to those described in **Table 1**. In addition, timing  
175 tephra loading to coincide with the maximum rate of  $C_{org}$  deposition at the sediment surface  
176 (e.g. following phytoplankton blooms) would further enhance the scale of  $C_{org}$  preservation.  
177 During seasonal upwelling, there is high  $C_{org}$  production in surface waters and fluxes to the

178 seafloor, but it is largely remineralised in oxygenated nature of the bottom waters, yielding low  
179 CBEs (Dale et al., 2015). Timing tephra delivery to just after the upwelling period may result  
180 in large absolute carbon burial.

### 181 **Resources required**

182 The only processing of the tephra prior to its use would be light crushing and sorting. Spreading  
183 tephra over the ocean would require infrastructure, including loading terminals and adapted  
184 ships (i.e. with mechanisms for tephra release), but land transport costs would be low because  
185 most volcanoes are located close to the oceans (Fig. 3). Marine vessels require an energy  
186 source, but the use of redundant coal barges could reduce CO<sub>2</sub> emissions. Freshly deposited  
187 tephra is unconsolidated and can be removed and loaded into transport using conventional  
188 excavators and trucks. In comparison to a number of other proposed GGR methods, this  
189 approach is uncomplicated (Table 2). Ocean fertilization, for example, requires the processing  
190 of Fe<sup>II</sup>-rich solution (Boyd et al., 2000), and other proposals require entirely new approaches  
191 to infrastructural development (e.g. carbon capture and storage; Royal Society, 2018). In  
192 contrast, offshore tephra addition would require; i) loading of ash onto barges; ii) travel to site  
193 of optimal loading as determined via study of seafloor environment and ocean currents (see  
194 Boyd et al., 2000); and iii) release of ash in a steady manner along prescribed paths.

### 195 **Environmental benefits and challenges**

196 Ocean-wide changes in bottom water and deep-sea oxygenation levels have been invoked as  
197 one of the causes of benthic foraminiferal extinction at the Cretaceous-Tertiary boundary (e.g.,  
198 Coccioni and Galeotti, 1994). Hence, it has been suggested that tephra deposition on the  
199 seafloor may have a similar on benthic communities. For example, ash fall associated with the  
200 1991 Mt. Pinatubo eruption caused mass mortality of benthic foraminifers over a large area of  
201 the South China Sea (Hess and Kuhnt, 1996), with mortality of all benthic foraminifers at sites  
202 receiving 6-8 cm of tephra. In addition, there was a reduction in species diversity at sites



203 receiving ~2 cm of tephra (Hess et al., 2001; Hess and Kuhnt, 1996). However, whereas  
204 recovery of the benthic community from the K-T extinction took several thousand years  
205 (Coccioni and Galeotti, 1994), recovery of South China Sea sediments was largely complete  
206 less than 10 years after tephra deposition, even in the areas that received the thickest deposits  
207 (Hess et al., 2001; Kuhnt et al., 2005). Tephra may leach some toxic elements into the water  
208 column (Jones and Gislason, 2008), and in some circumstances can lead to a drop in the pH of  
209 seawater as acids are released (Frogner Kockum et al., 2006; Frogner et al., 2001). Other  
210 impacts of tephra deposition are unknown, including potential impacts on planktic, and larger  
211 organisms. However, while large scale tephra input to surface waters in the immediate vicinity  
212 of volcanoes may be harmful, there is no evidence that the initial mortality is long-lasting or  
213 widespread (Hoffmann et al., 2012; Jones and Gislason, 2008; Wall-Palmer et al., 2011). There  
214 are also examples from the geologic record showing that pre-deposition benthic ostracod  
215 species survived at least 6 cm of tephra deposition (Perrier et al., 2012). Nevertheless,  
216 environmental impact assessments would be required to examine ecosystem responses to  
217 enhanced tephra loading.

218 Tephra extraction will lead to environmental impacts on-shore, but most types of tephra are of  
219 low toxicity and the risks can be mitigated by standard procedures such as cast-back mining  
220 adopted during industrial bentonite extraction (Eisenhour and Brown, 2009).

### 221 **Scalability and engineering challenges**

222 As with ocean fertilization through iron addition, tephra fertilization should be scalable without  
223 significant cost increases. The financial cost/benefit ratio depends on the scale of operations  
224 and the site selection. Typical charter rates for 50,000 t bulk carriers are ~\$10,000 d<sup>-1</sup> which,  
225 for a 2000 km deployment at 20 km hr<sup>-1</sup> and 2 days loading (UNCTAD, 2018), yields a cost of  
226 ~\$70,000 per deployment. Terrestrial transport costs will increase this estimate. If we assume  
227 ~\$600 d<sup>-1</sup> to hire a 44-tonne truck, and ten 60-km round journeys are possible per day, then

228 ~\$68,000 will be necessary per deployment. Even so, the estimated cost of \$55 per tCO<sub>2</sub>  
229 deployed, based on the estimates in [Table 1](#), is an order of magnitude lower than many other  
230 GGR technologies ([Table 2](#), [Royal Society, 2018](#)).

### 231 **Monitoring and evaluation**

232 Many of the risks to implementation and optimization of tephra dispersal can be investigated  
233 in laboratory studies. Both natural (e.g. [Hamme et al., 2010](#); [Langmann et al., 2010](#); [Olgun et](#)  
234 [al., 2011](#)) and laboratory studies (e.g. [Hoffmann et al., 2012](#); [Mélançon et al., 2014](#)) have shown  
235 that ash fertilizes phytoplankton productivity, so the primary risk is that the approach does not  
236 sufficiently raise CBEs. This question may be tackled by undertaking experiments to measure  
237 C<sub>org</sub> degradation rates under various conditions of tephra loading and over a range of sediment  
238 types. The responses of benthic biota to tephra loading can also be investigated in laboratory  
239 studies (cf. [Brown et al., 2017](#)). Once laboratory tests are completed, small-scale *in situ* studies  
240 would be necessary to test the concept, with several years of monitoring.

### 241 **Social factors**

242 Natural volcanic processes transport millions of tonnes of tephra to the oceans every year, with  
243 an estimated  $2.2 \times 10^8$  t yr deposited in the Pacific Ocean alone ([Olgun et al., 2011](#)). Hence,  
244 unlike most other proposed GGR interventions, the mechanism outlined here is an  
245 augmentation to a naturally occurring process. In addition, tephra addition to the ocean does  
246 not require changes to land use, such as reforestation of agricultural land. Freshly deposited  
247 tephra frequently creates a barren landscape in volcanic areas, and following eruptions  
248 governments may have to invest funds to clear tephra from local infrastructure. Hence, tephra  
249 deposits can be seen as a problem that requires a solution. Nevertheless, public opinion  
250 regarding any GGR initiative is likely to be mixed ([Royal Society, 2018](#)), and it would be  
251 important to undertake public engagement to communicate the positive aspects of the approach.

252       **Policy factors**

253       The ‘dumping’ of material in international waters is currently banned under the London  
254       Convention and Protocol, but the restriction of tephra loading to shallow waters within  
255       territorial waters of individual nations is less clear and would require clarification.

256       **Conclusions**

257       We have outlined how artificial addition of tephra to the ocean may lead to C<sub>org</sub> sequestration  
258       and GGR, and have discussed its positive and negative aspects. The advantages of tephra  
259       dispersal in this regard are:

- 260       • tephra addition to the oceans is a natural process
- 261       • tephra is widely distributed around the world
- 262       • the technology is simple and readily available
- 263       • no repurposing of valuable land resources is required
- 264       • tephra is not a scarce resource

265       The key factors required to transform this hypothesis into a potentially viable GGR method  
266       are:

- 267       • optimization to achieve maximum GGR for minimal tephra loading
- 268       • identification of optimal oceanic sites
- 269       • determination of potential ecological impacts
- 270       • assessment of prime locations for sourcing tephra and optimal approaches for  
271       transporting tephra to the ocean
- 272       • assessment of the scalability and economics required to have a significant GGR impact

273       Based on this analysis, we suggest there is a prima facie case for further study of tephra addition  
274       to the oceans as part of the palette of strategies to achieve GGR.

275 **References**

- 276 Arthur, M.A., Dean, W.E., Laarkamp, K., 1998. Organic carbon accumulation and  
277 preservation in surface sediments on the Peru margin. *Chem. Geol.* 152, 273–286.  
278 [https://doi.org/10.1016/S0009-2541\(98\)00120-X](https://doi.org/10.1016/S0009-2541(98)00120-X)
- 279 Bastin, J.-F., Finegold, Y., Garcia, C., Mollicone, D., Rezende, M., Routh, D., Zohner, C.M.,  
280 Crowther, T.W., 2019. The global tree restoration potential. *Science* (80-. ). 365, 76–79.  
281 <https://doi.org/10.1126/SCIENCE.AAX0848>
- 282 Bohlen, L., Dale, A.W., Sommer, S., Mosch, T., Hensen, C., Noffke, A., Scholz, F.,  
283 Wallmann, K., 2011. Benthic nitrogen cycling traversing the Peruvian oxygen minimum  
284 zone. *Geochim. Cosmochim. Acta* 75, 6094–6111.  
285 <https://doi.org/10.1016/j.gca.2011.08.010>
- 286 Boyd, P.W., Jickells, T., Law, C.S., Blain, S., Boyle, E.A., Buesseler, K.O., Coale, K.H.,  
287 Cullen, J.J., de Baar, H.J.W., Follows, M., Harvey, M., Lancelot, C., Levasseur, M.,  
288 Owens, N.P.J., Pollard, R., Rivkin, R.B., Sarmiento, J., Schoemann, V., Smetacek, V.,  
289 Takeda, S., Tsuda, A., Turner, S., Watson, A.J., 2007. Mesoscale iron enrichment  
290 experiments 1993-2005: synthesis and future directions. *Science* 315, 612–7.  
291 <https://doi.org/10.1126/science.1131669>
- 292 Boyd, P.W., Watson, A.J., Law, C.S., Abraham, E.R., Trull, T., Murdoch, R., Bakker,  
293 D.C.E., Bowie, A.R., Buesseler, K.O., Chang, H., Charette, M., Croot, P., Downing, K.,  
294 Frew, R., Gall, M., Hadfield, M., Hall, J., Harvey, M., Jameson, G., LaRoche, J.,  
295 Liddicoat, M., Ling, R., Maldonado, M.T., McKay, R.M., Nodder, S., Pickmere, S.,  
296 Pridmore, R., Rintoul, S., Safi, K., Sutton, P., Strzepek, R., Tanneberger, K., Turner, S.,  
297 Waite, A., Zeldis, J., 2000. A mesoscale phytoplankton bloom in the polar Southern  
298 Ocean stimulated by iron fertilization. *Nature* 407, 695–702.

299 <https://doi.org/10.1038/35037500>

300 Brown, A., Thatje, S., Hauton, C., 2017. The Effects of Temperature and Hydrostatic  
301 Pressure on Metal Toxicity: Insights into Toxicity in the Deep Sea. *Environ. Sci.*  
302 *Technol.* 51, 10222–10231. <https://doi.org/10.1021/acs.est.7b02988>

303 Burdige, D.J., 2007. Preservation of organic matter in marine sediments: Controls,  
304 mechanisms, and an imbalance in sediment organic carbon budgets? *Chem. Rev.* 107,  
305 467–485. <https://doi.org/10.1021/cr050347q>

306 Coccioni, R., Galeotti, S., 1994. K-T boundary extinction: geologically instantaneous or  
307 gradual event? Evidence from deep-sea benthic foraminifera. *Geology* 22, 779–782.  
308 [https://doi.org/10.1130/0091-7613\(1994\)022<0779:KTBEGI>2.3.CO;2](https://doi.org/10.1130/0091-7613(1994)022<0779:KTBEGI>2.3.CO;2)

309 Dale, A.W., Sommer, S., Lomnitz, U., Montes, I., Treude, T., Liebetrau, V., Gier, J., Hensen,  
310 C., Dengler, M., Stolpovsky, K., Bryant, L.D., Wallmann, K., 2015. Organic carbon  
311 production, mineralisation and preservation on the Peruvian margin. *Biogeosciences* 12,  
312 1537–1559. <https://doi.org/10.5194/bg-12-1537-2015>

313 Duggen, S., Croot, P., Schacht, U., Hoffmann, L., 2007. Subduction zone volcanic ash can  
314 fertilize the surface ocean and stimulate phytoplankton growth: Evidence from  
315 biogeochemical experiments and satellite data. *Geophys. Res. Lett.* 34, L01612.  
316 <https://doi.org/10.1029/2006GL027522>

317 Duggen, S., Olgun, N., Croot, P., Hoffmann, L., Dietze, H., Delmelle, P., Teschner, C.,  
318 Skolen, A.P.M., 2010. The role of airborne volcanic ash for the surface ocean  
319 biogeochemical iron-cycle: a review, *Biogeosciences*.

320 Dunne, J.P., Sarmiento, J.L., Gnanadesikan, A., 2007. A synthesis of global particle export  
321 from the surface ocean and cycling through the ocean interior and on the seafloor.

322 Global Biogeochem. Cycles 21, n/a-n/a. <https://doi.org/10.1029/2006GB002907>

323 Eisenhour, D.D., Brown, R.K., 2009. Bentonite and its impact on modern life. *Elements*.

324 <https://doi.org/10.2113/gselements.5.2.83>

325 Falkowski, P., Scholes, P.J., Boyle, E., Canadell, J., Canfield, D., Elser, J., Gruber, N.,

326 Hibbard, K., Högberg, P., Linder, S., Mackenzie, F.T., Moore III, B., Pedersen, T.,

327 Rosenthal, Y., Seitzinger, S., Smetacek, V., Steffen, W., 2000. The Global Carbon

328 Cycle: A Test of Our Knowledge of Earth as a System. *Science* (80-. ). 290, 291–296.

329 <https://doi.org/10.1126/science.274.5291.1346>

330 Frogner Kockum, P.C., Herbert, R.B., Gislason, S.R., 2006. A diverse ecosystem response to

331 volcanic aerosols. *Chem. Geol.* 231, 57–66.

332 <https://doi.org/10.1016/j.chemgeo.2005.12.008>

333 Frogner, P., Reynir Gíslason, S., Óskarsson, N., 2001. Fertilizing potential of volcanic ash in

334 ocean surface water. *Geology* 29, 487. [https://doi.org/10.1130/0091-](https://doi.org/10.1130/0091-7613(2001)029<0487:FPOVAI>2.0.CO;2)

335 [7613\(2001\)029<0487:FPOVAI>2.0.CO;2](https://doi.org/10.1130/0091-7613(2001)029<0487:FPOVAI>2.0.CO;2)

336 Ghouleh, Z., Guthrie, R.I.L., Shao, Y., 2017. Production of carbonate aggregates using steel

337 slag and carbon dioxide for carbon-negative concrete. *J. CO2 Util.* 18, 125–138.

338 <https://doi.org/10.1016/j.jcou.2017.01.009>

339 Gieskes, J.M., 1983. The chemistry of interstitial waters of deep sea sediments: interpretation

340 of deep sea drilling data, in: Riley, J.P., Chester, R. (Eds.), *Chemical Oceanography*.

341 Academic Press, London, pp. 221–269.

342 Gudmundsson, M.T., Thordarson, T., Höskuldsson, Á., Larsen, G., Björnsson, H., Prata, F.J.,

343 Oddsson, B., Magnússon, E., Högnadóttir, T., Petersen, G.N., Hayward, C.L.,

344 Stevenson, J.A., Jónsdóttir, I., 2012. Ash generation and distribution from the April-May

345 2010 eruption of Eyjafjallajökull, Iceland. *Sci. Rep.* 2, 572.  
346 <https://doi.org/10.1038/srep00572>

347 Haeckel, M., van Beusekom, J., Wiesner, M.G., König, I., 2001. The impact of the 1991  
348 Mount Pinatubo tephra fallout on the geochemical environment of the deep-sea  
349 sediments in the South China Sea. *Earth Planet. Sci. Lett.* 193, 151–166.  
350 [https://doi.org/10.1016/S0012-821X\(01\)00496-4](https://doi.org/10.1016/S0012-821X(01)00496-4)

351 Hamme, R.C., Webley, P.W., Crawford, W.R., Whitney, F.A., DeGrandpre, M.D., Emerson,  
352 S.R., Eriksen, C.C., Giesbrecht, K.E., Gower, J.F.R., Kavanaugh, M.T., Peña, M.A.,  
353 Sabine, C.L., Batten, S.D., Coogan, L.A., Grundle, D.S., Lockwood, D., 2010. Volcanic  
354 ash fuels anomalous plankton bloom in subarctic northeast Pacific. *Geophys. Res. Lett.*  
355 37, n/a-n/a. <https://doi.org/10.1029/2010GL044629>

356 Hartnett, H.E., Keil, R.G., Hedges, J.I., Devol, A.H., 1998. Influence of oxygen exposure  
357 time on organic carbon preservation in continental margin sediments. *Nature* 391, 572–  
358 575. <https://doi.org/10.1038/35351>

359 Haszeldine, R.S., Flude, S., Johnson, G., Scott, V., 2018. Negative emissions technologies  
360 and carbon capture and storage to achieve the Paris Agreement commitments. *Philos.*  
361 *Trans. R. Soc. A Math. Eng. Sci.* 376, 20160447. <https://doi.org/10.1098/rsta.2016.0447>

362 Hembury, D.J., Palmer, M.R., Fones, G.R., Mills, R.A., Marsh, R., Jones, M.T., 2012.  
363 Uptake of dissolved oxygen during marine diagenesis of fresh volcanic material.  
364 *Geochim. Cosmochim. Acta* 84, 353–368. <https://doi.org/10.1016/J.GCA.2012.01.017>

365 Hess, S., Kuhnt, W., 1996. Deep-sea benthic foraminiferal recolonization of the 1991 Mt.  
366 Pinatubo ash layer in the South China Sea. *Mar. Micropaleontol.* 28, 171–197.  
367 [https://doi.org/10.1016/0377-8398\(95\)00080-1](https://doi.org/10.1016/0377-8398(95)00080-1)

368 Hess, S., Kuhnt, W., Hill, S., Kaminski, M.A., Holbourn, A., de Leon, M., 2001. Monitoring  
369 the recolonization of the Mt Pinatubo 1991 ash layer by benthic foraminifera. *Mar.*  
370 *Micropaleontol.* 43, 119–142. [https://doi.org/10.1016/S0377-8398\(01\)00025-1](https://doi.org/10.1016/S0377-8398(01)00025-1)

371 Hoffmann, L.J., Breitbarth, E., Ardelan, M.V., Duggen, S., Olgun, N., Hassellöv, M.,  
372 Wängberg, S.-Å., 2012. Influence of trace metal release from volcanic ash on growth of  
373 *Thalassiosira pseudonana* and *Emiliana huxleyi*. *Mar. Chem.* 132–133, 28–33.  
374 <https://doi.org/10.1016/J.MARCHEM.2012.02.003>

375 Homoky, W.B., Hembury, D.J., Hepburn, L.E., Mills, R.A., Statham, P.J., Fones, G.R.,  
376 Palmer, M.R., 2011. Iron and manganese diagenesis in deep sea volcanogenic sediments  
377 and the origins of pore water colloids. *Geochim. Cosmochim. Acta* 75, 5032–5048.  
378 <https://doi.org/10.1016/J.GCA.2011.06.019>

379 IPCC, 2018. Summary for Policymakers, in: Masson-Delmotte, V., Zhai, P., Pörtner, H.O.,  
380 Roberts, D., Skea, J., Shukla, P.R., Pirani, A., Chen, Y., Connors, S., Gomis, M.,  
381 Lonnoy, E., Matthews, J.B.R., Moufouma-Okia, W., Péan, C., Pidcock, R., Reay, N.,  
382 Tignor, M., Waterfield, T., Zhou, X. (Eds.), *Global Warming of 1.5°C. An IPCC Special*  
383 *Report on the Impacts of Global Warming of 1.5°C above Pre-Industrial Levels and*  
384 *Related Global Greenhouse Gas Emission Pathways, in the Context of Strengthening the*  
385 *Global Response to the Threat of Climate Change.*, World Meteorological Organization,  
386 Geneva, p. 32. <https://doi.org/10.1017/CBO9781107415324>

387 Jones, M.T., Gislason, S.R., 2008. Rapid releases of metal salts and nutrients following the  
388 deposition of volcanic ash into aqueous environments. *Geochim. Cosmochim. Acta* 72,  
389 3661–3680. <https://doi.org/10.1016/j.gca.2008.05.030>

390 Kheshgi, H.S., 1995. Sequestering atmospheric carbon dioxide by increasing ocean alkalinity.  
391 *Energy* 20, 915–922. [https://doi.org/10.1016/0360-5442\(95\)00035-F](https://doi.org/10.1016/0360-5442(95)00035-F)



392 Kuhnt, W., Hess, S., Holbourn, A., Paulsen, H., Salomon, B., 2005. The impact of the 1991  
393 Mt. Pinatubo eruption on deep-sea foraminiferal communities: A model for the  
394 Cretaceous–Tertiary (K/T) boundary? *Palaeogeogr. Palaeoclimatol. Palaeoecol.* 224,  
395 83–107. <https://doi.org/10.1016/J.PALAEO.2005.03.042>

396 Lalonde, K., Mucci, A., Ouellet, A., Gélinas, Y., 2012. Preservation of organic matter in  
397 sediments promoted by iron. *Nature* 483, 198–200. <https://doi.org/10.1038/nature10855>

398 Langmann, B., Zakšek, K., Hort, M., Duggen, S., 2010. Volcanic ash as fertiliser for the  
399 surface ocean, *Atmos. Chem. Phys.*

400 Lin, I.I., Hu, C., Li, Y.H., Ho, T.Y., Fischer, T.P., Wong, G.T.F., Wu, J., Huang, C.W., Chu,  
401 D.A., Ko, D.S., Chen, J.P., 2011. Fertilization potential of volcanic dust in the low-  
402 nutrient low-chlorophyll western North Pacific subtropical gyre: Satellite evidence and  
403 laboratory study. *Global Biogeochem. Cycles* 25.  
404 <https://doi.org/10.1029/2009GB003758>

405 Lomax, G., Workman, M., Lenton, T., Shah, N., 2015. Reframing the policy approach to  
406 greenhouse gas removal technologies. *Energy Policy* 78, 125–136.  
407 <https://doi.org/10.1016/j.enpol.2014.10.002>

408 Longman, J., Palmer, M.R., Gernon, T.M., Manners, H.R., 2019. The role of tephra in  
409 enhancing organic carbon preservation in marine sediments. *Earth-Science Rev.*  
410 <https://doi.org/10.1016/J.EARSCIREV.2019.03.018>

411 Martin, J.H., Fitzwater, S.E., 1988. Iron deficiency limits phytoplankton growth in the north-  
412 east pacific subarctic. *Nature* 331, 341–343. <https://doi.org/10.1038/331341a0>

413 Maters, E.C., Delmelle, P., Gunnlaugsson, H.P., 2017. Controls on iron mobilisation from  
414 volcanic ash at low pH: Insights from dissolution experiments and Mössbauer

415 spectroscopy. *Chem. Geol.* 449, 73–81.  
416 <https://doi.org/10.1016/J.CHEMGEO.2016.11.036>

417 Mathers, J., Craft, E., Norsworthy, M., Wolfe, C., 2014. *Green Freight Handbook*.  
418 Environmental Defense Fund, New York.

419 Matter, J.M., Stute, M., Snæbjörnsdóttir, S.Ó., Oelkers, E.H., Gislason, S.R., Aradóttir, E.S.,  
420 Sigfusson, B., Gunnarsson, I., Sigurdardóttir, H., Gunnlaugsson, E., Axelsson, G.,  
421 Alfredsson, H.A., Wolff-Boenisch, D., Mesfin, K., Fernandez de la Reguera Taya, D.,  
422 Hall, J., Dideriksen, K., Broecker, W.S., 2016. Rapid carbon mineralization for  
423 permanent disposal of anthropogenic carbon dioxide emissions. *Science* 352, 1312–4.  
424 <https://doi.org/10.1126/science.aad8132>

425 Mélançon, J., Levasseur, M., Lizotte, M., Delmelle, P., Cullen, J., Hamme, R.C., Peña, A.,  
426 Simpson, K.G., Scarratt, M., Tremblay, J.-É.É., Zhou, J., Johnson, K., Sutherland, N.,  
427 Arychuk, M., Nemcek, N., Robert, M., 2014. Early response of the northeast subarctic  
428 Pacific plankton assemblage to volcanic ash fertilization. *Limnol. Oceanogr.* 59, 55–67.  
429 <https://doi.org/10.4319/lo.2014.59.1.0055>

430 Murray, N.A., McManus, J., Palmer, M.R., Haley, B., Manners, H., 2018. Diagenesis in  
431 tephra-rich sediments from the Lesser Antilles Volcanic Arc: Pore fluid constraints.  
432 *Geochim. Cosmochim. Acta* 228, 119–135. <https://doi.org/10.1016/J.GCA.2018.02.039>

433 Olgun, N., Duggen, S., Croot, P.L., Delmelle, P., Dietze, H., Schacht, U., Óskarsson, N.,  
434 Siebe, C., Auer, A., Garbe-Schönberg, D., 2011. Surface ocean iron fertilization: The  
435 role of airborne volcanic ash from subduction zone and hot spot volcanoes and related  
436 iron fluxes into the Pacific Ocean. *Global Biogeochem. Cycles* 25, n/a-n/a.  
437 <https://doi.org/10.1029/2009GB003761>

438 Pabortsava, K., Lampitt, R.S., Benson, J., Crowe, C., McLachlan, R., Le Moigne, F.A.C.,

439 Mark Moore, C., Pebody, C., Provost, P., Rees, A.P., Tilstone, G.H., Woodward,  
440 E.M.S., 2017. Carbon sequestration in the deep Atlantic enhanced by Saharan dust. *Nat.*  
441 *Geosci.* 10, 189–194. <https://doi.org/10.1038/ngeo2899>

442 Pennington, J.T., Mahoney, K.L., Kuwahara, V.S., Kolber, D.D., Calienes, R., Chavez, F.P.,  
443 2006. Primary production in the eastern tropical Pacific: A review. *Prog. Oceanogr.* 69,  
444 285–317. <https://doi.org/10.1016/j.pocean.2006.03.012>

445 Perrier, V., Meidla, T., Tinn, O., Ainsaar, L., 2012. Biotic response to explosive volcanism:  
446 Ostracod recovery after Ordovician ash-falls. *Palaeogeogr. Palaeoclimatol. Palaeoecol.*  
447 365–366, 166–183. <https://doi.org/10.1016/j.palaeo.2012.09.024>

448 Ramage, M.H., Burridge, H., Busse-Wicher, M., Fereday, G., Reynolds, T., Shah, D.U., Wu,  
449 G., Yu, L., Fleming, P., Densley-Tingley, D., Allwood, J., Dupree, P., Linden, P.F.,  
450 Scherman, O., 2017. The wood from the trees: The use of timber in construction.  
451 *Renew. Sustain. Energy Rev.* <https://doi.org/10.1016/j.rser.2016.09.107>

452 Renforth, P., Henderson, G., 2017. Assessing ocean alkalinity for carbon sequestration. *Rev.*  
453 *Geophys.* 55, 636–674. <https://doi.org/10.1002/2016RG000533>

454 Royal Society, T., 2018. Greenhouse Gas Removal. Royal Society, London.

455 Rubin, M., Berman-Frank, I., Shaked, Y., 2011. Dust- and mineral-iron utilization by the  
456 marine dinitrogen-fixer *Trichodesmium*. *Nat. Geosci.* 4, 529–534.  
457 <https://doi.org/10.1038/ngeo1181>

458 Sarmiento, J.L., Gruber, N., 2006. Ocean biogeochemical dynamics. Princeton University  
459 Press.

460 Schrag, D.P., Higgins, J.A., Macdonald, F.A., Johnston, D.T., 2013. Authigenic carbonate  
461 and the history of the global carbon cycle. *Science* (80-. ). 339, 540–3.

462 <https://doi.org/10.1126/science.1229578>

463 Scudder, R.P., Murray, R.W., Schindlbeck, J.C., Kutterolf, S., Hauff, F., Underwood, M.B.,  
464 Gwizd, S., Lauzon, R., McKinley, C.C., 2016. Geochemical approaches to the  
465 quantification of dispersed volcanic ash in marine sediment. *Prog. Earth Planet. Sci.* 3,  
466 1. <https://doi.org/10.1186/s40645-015-0077-y>

467 Siegenthaler, U., Sarmiento, J.L., 1993. Atmospheric carbon dioxide and the ocean. *Nature*.  
468 <https://doi.org/10.1038/365119a0>

469 Steffen, W., Rockström, J., Richardson, K., Lenton, T.M., Folke, C., Liverman, D.,  
470 Summerhayes, C.P., Barnosky, A.D., Cornell, S.E., Crucifix, M., Donges, J.F., Fetzer,  
471 I., Lade, S.J., Scheffer, M., Winkelmann, R., Schellnhuber, H.J., 2018. Trajectories of  
472 the Earth System in the Anthropocene. *Proc. Natl. Acad. Sci.* 115, 8252–8259.  
473 <https://doi.org/10.1073/pnas.1810141115>

474 Tollefson, J., 2018. IPCC says limiting global warming to 1.5 °C will require drastic action.  
475 *Nature* 562, 172–173. <https://doi.org/10.1038/d41586-018-06876-2>

476 Uematsu, M., Toratani, M., Kajino, M., Narita, Y., Senga, Y., Kimoto, T., 2004.  
477 Enhancement of primary productivity in the western North Pacific caused by the  
478 eruption of the Miyake-jima Volcano. *Geophys. Res. Lett.* 31, n/a-n/a.  
479 <https://doi.org/10.1029/2003gl018790>

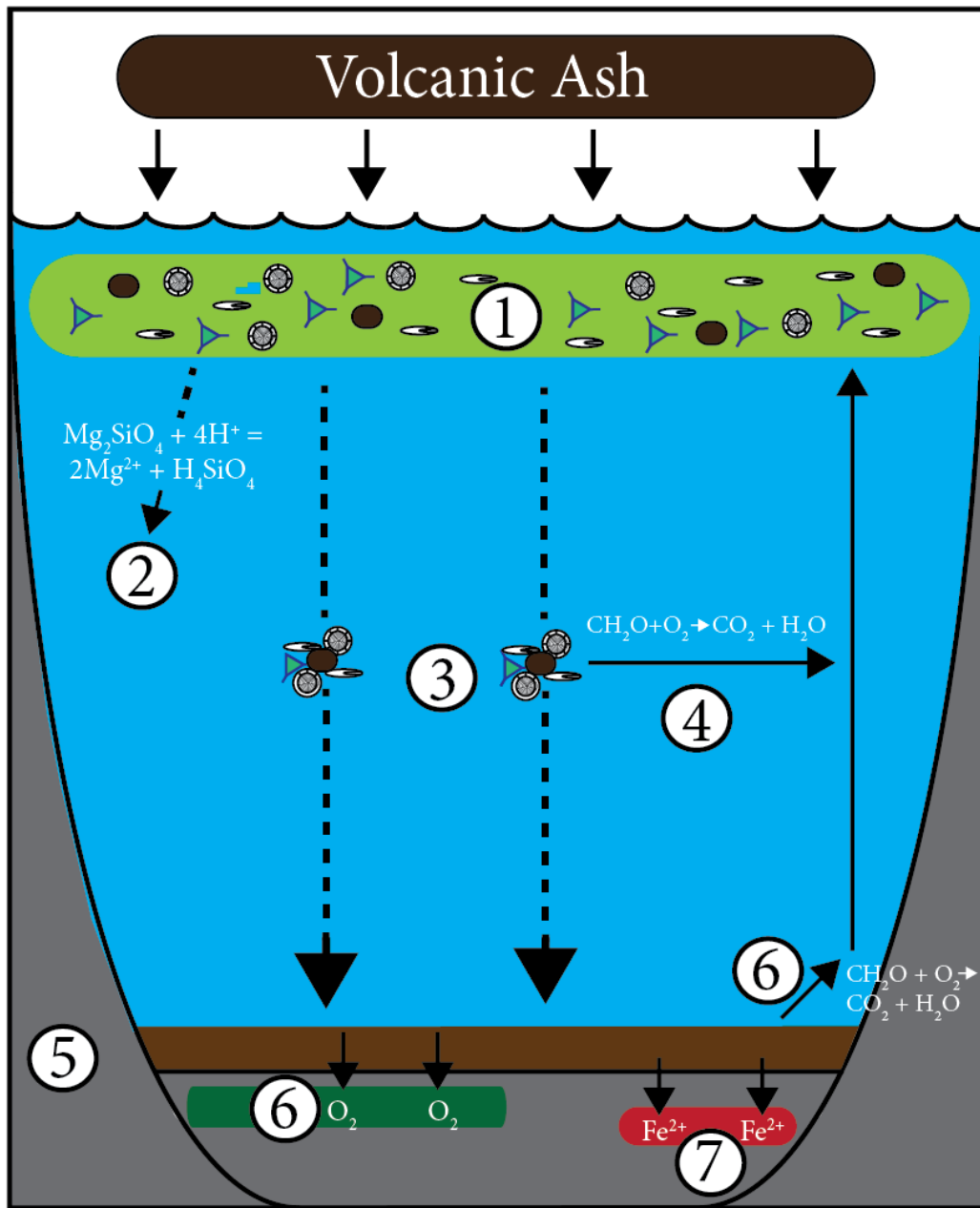
480 UNCTAD, 2018. *Review of Maritime Transport*. United Nations, New York and Geneva.

481 Wall-Palmer, D., Jones, M.T., Hart, M.B., Fisher, J.K., Smart, C.W., Hembury, D.J., Palmer,  
482 M.R., Fones, G.R., 2011. Explosive volcanism as a cause for mass mortality of  
483 pteropods. *Mar. Geol.* 282, 231–239. <https://doi.org/10.1016/J.MARGEO.2011.03.001>

484 Zahariev, K., Christian, J.R., Denman, K.L., 2008. Preindustrial, historical, and fertilization

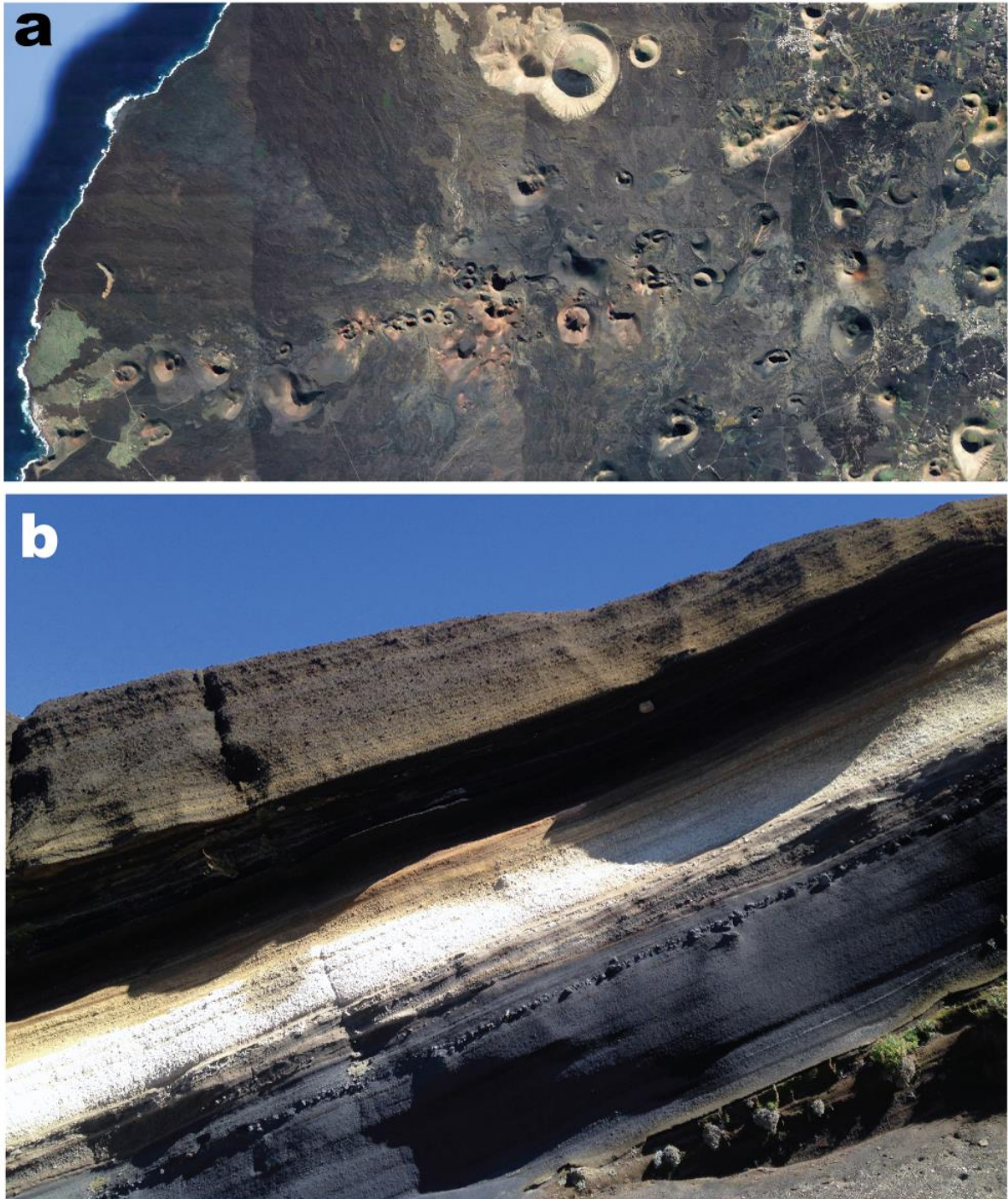
485 simulations using a global ocean carbon model with new parameterizations of iron  
486 limitation, calcification, and N2 fixation. Prog. Oceanogr. 77, 56–82.  
487 <https://doi.org/10.1016/j.pocean.2008.01.007>

488 **Figures**



489  
490 **Figure 1:** Schematic image detailing the processes which may occur to enhance carbon sequestration  
491 and greenhouse gas removal via the addition of volcanic ash to the ocean. 1) The fertilization of  
492 phytoplankton blooms in the upper ocean. 2) The release of  $Mg^{2+}$  (and  $Ca^{2+}$ ) ions to the ocean, via the  
493 dissolution of minerals contained in the ash. Here we use the dissolution of olivine as an example.  
494  $Mg^{2+}$  are released during this process which consumes  $H^+$  ions, thus increasing alkalinity. 3) The  
495 transfer of organic carbon from the upper to lower ocean (the biological pump), enhanced by the

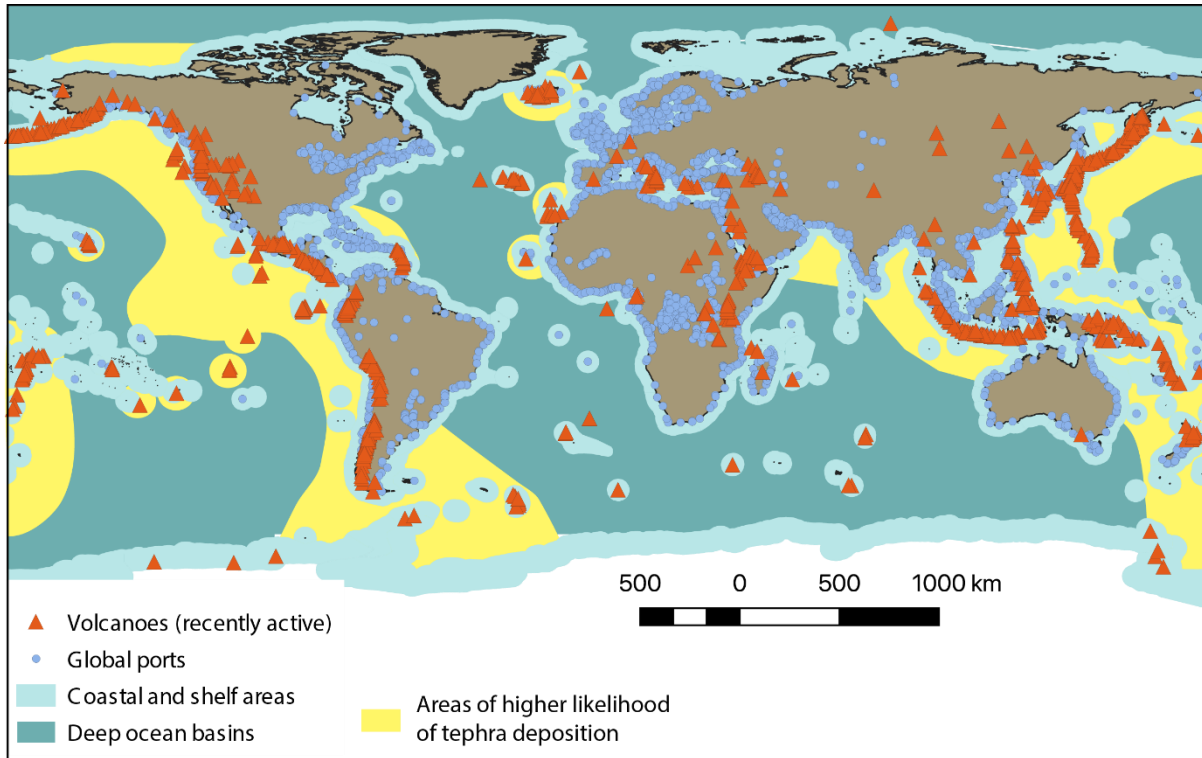
496 association of phytoplankton to ash particles. 4) The remineralization of some organic matter during  
497 transport through an oxygenated water column 5) The formation of a volcanic ash layer at the  
498 sediment-water interface. 6) Removal of O<sub>2</sub> from organic-rich sediments and formation of anoxic  
499 conditions, reducing organic carbon oxidation and remineralization. 7) The release of reactive species  
500 of Fe, Mn and Al, available to bind to organic carbon and reduce oxidation.



501

502 **Figure 2:** Examples of Holocene-age tephra in the natural environment. Panel a is an aerial image of  
503 cinder cone volcanoes in Lanzarote (Canary Islands), displaying both the extensive tephra fields  
504 surrounding them and their proximity to the ocean. Panel b is an example of bedded tephra deposits  
505 from Tenerife (also Canary Islands).





506

507 **Figure 3:** Global map displaying the location of all active (and recently active) volcanoes (red  
 508 triangles), and of global ports (blue circles) Also indicated is regions in which tephra deposition is  
 509 considered highly likely (yellow), from [Olgun et al., 2011](#). Most volcanoes are located either on, or  
 510 close to the ocean, and very few are a significant distance from major ports. Also displayed are the  
 511 extent of coastal and shelf seas (those which are <200 m in depth), which would be the target for  
 512 offshore tephra addition.

513

514

515 **Table 1:** Estimates of gross and net potential CO<sub>2</sub> storage. <sup>a</sup> Typical CO<sub>2</sub> equivalent fluxes are  
516 calculated from the POC rain rate of Site 1 from the inner Peruvian shelf (Dale et al., 2015). <sup>b</sup> Burial  
517 efficiencies are taken from the average carbon burial efficiency of sites 1 and 2 of the inner Peru shelf,  
518 with OMZ carbon burial efficiencies an average of sites 6-8 (Dale et al., 2015). <sup>c</sup> Mass of tephra with  
519 a density of 1400 kg m<sup>3</sup> (a typical value of tephra; Gudmundsson et al., 2012) and 50 % porosity  
520 (Hembury et al., 2012) required per square meter of seafloor. <sup>d</sup> Bulk carrier capacity from Freese,  
521 2017. <sup>e</sup> Yearly CO<sub>2</sub> equivalent flux to the area covered by tephra. <sup>f</sup> Gross increase in CO<sub>2</sub> preserved in  
522 sediment achieved by reducing remineralization by 29%. <sup>g</sup> Estimate of onshore CO<sub>2</sub> emissions,  
523 calculated assuming truck size of 44 tonnes (typical articulated lorry load size) an average distance of  
524 30km from tephra source to port, 1140 journeys necessary to carry 50,000 tonnes of tephra, and using  
525 the EDF's green freight calculator (Mathers et al., 2014). <sup>h</sup> Estimate of offshore CO<sub>2</sub> emissions,  
526 calculated from values in Freese, 2017. <sup>j</sup> Net CO<sub>2</sub> storage calculated via subtraction of onshore and  
527 offshore CO<sub>2</sub> emissions from gross storage.

528

| <b>Gross potential CO<sub>2</sub> storage</b>   | <b>Value</b>  |
|---|---|
| Typical inner Peru shelf C <sub>org</sub> burial rate                                       | 79.5 mmol m <sup>-2</sup> d <sup>-1</sup> <sup>a</sup>              |
| Yearly C <sub>org</sub> flux to sediments   | 348.52 gC m <sup>-2</sup> yr <sup>-1</sup> <sup>a</sup>             |
| CO <sub>2</sub> equivalent flux to sediments  | 1277 gCO <sub>2</sub> m <sup>-2</sup> yr <sup>-1</sup> <sup>a</sup> |
| Typical Peru shelf burial efficiency  | 18% <sup>b</sup>  |
| Typical Peru shelf burial efficiency below Oxygen Minimum Zone                              | 47 % <sup>b</sup>   |
| Likely increase in burial efficiency as a result of O <sub>2</sub> depletion                | 29% <sup>b</sup>  |
| <b>Resource requirement</b>   |   |
| Thickness of tephra applied to sediment   | 0.5 cm  |
| Volume of tephra required per square meter  | 5 x 10 <sup>3</sup> cm <sup>3</sup> m <sup>-2</sup>                 |
| Mass of tephra (50% porosity)   | 6.7 x 10 <sup>3</sup> g m <sup>-2</sup> <sup>c</sup>                |
| Assumed bulk carrier capacity   | 50,000 t <sup>d</sup>   |
| Area covered per carrier load   | 7.5 x 10 <sup>6</sup> m <sup>2</sup> <sup>c</sup>                   |
| Yearly supply of carbon to this area before remineralization                                | 2.61 x 10 <sup>9</sup> gC yr <sup>-1</sup> <sup>e</sup>             |
| <b>Gross CO<sub>2</sub> storage per load per year for 29% reduction of remineralization</b> | <b>2777 t CO<sub>2</sub> <sup>f</sup></b>                           |
| <b>CO<sub>2</sub> emissions associated</b>  |   |
| CO <sub>2</sub> emitted by 44 tonne truck (per tonne load and km travelled)                 | 91.2 gCO <sub>2</sub> t <sup>-1</sup> km <sup>-1</sup> <sup>g</sup> |
| Distance from tephra source to port   | 30 km <sup>g</sup>  |
| Number of journeys  | ~1140 <sup>g</sup>  |
| CO <sub>2</sub> emitted per 50,000 tonnes tephra transported to port                        | 136 t CO <sub>2</sub> <sup>g</sup>                                  |



|  |  |
|--|--|
| CO <sub>2</sub> emitted by carrier (per tonne load and km travelled) | 3 gCO <sub>2</sub> t <sup>-1</sup> km <sup>-1</sup> <sup>h</sup>     |
| CO <sub>2</sub> emitted by 50,000 t bulk carrier                     | 150 x 10 <sup>3</sup> gCO <sub>2</sub> km <sup>-1</sup> <sup>h</sup> |
| Distance to and from load port, and tephra spreading                 | 2000 km <sup>i</sup>   |
| CO <sub>2</sub> emitted per carrier load                             | 300 t CO <sub>2</sub> <sup>h</sup>                                   |
| <b>Net CO<sub>2</sub> storage per load</b>                           | <b>2341 t CO<sub>2</sub> <sup>j</sup></b>                            |

529

530 Table 2: Comparison of removal potential and costs, alongside technology readiness levels (TRLs) of  
531 other proposed GGR methods, and enhanced tephra loading. Table adapted from [Royal Society](#)  
532 [\(2018\)](#), with additional data from this study. <sup>a</sup> Estimates of global potential for CO<sub>2</sub> removal from  
533 tephra loading taken from [Longman et al. \(2019\)](#). There are 9 TRLs describing maturity of  
534 technology: TRL1 basic principles, TRL2 invention and research, TRL3 proof of concept, TRL4  
535 bench scale research, TRL5 pilot scale, TRL6 large scale, TRL7 inactive commissioning, TRL8 active  
536 commissioning and TRL9 operations.

| <b><u>GGR Method</u></b>                           | <b><u>Global CO<sub>2</sub> removal potential (Gt CO<sub>2</sub> a<sup>-1</sup>)</u></b> | <b><u>Cost per tCO<sub>2</sub> (US\$)</u></b>    | <b><u>Technology readiness level (TRL)</u></b> |
|--|--|--|--|
| Afforestation, reforestation and forest management | Afforestation/reforestation: 3-20, forest management: 1-2                                | 3-30   | 8-9  |
| Wetland, peatland and coastal habitat restoration  | 0.4-20   | 10-100   | 5-6  |
| Soil carbon sequestration                          | 1-10   | 10 profit, 3 cost                                | 8-9  |
| Biochar  | 2-5  | 0-200  | 3-6  |
| Ocean fertilization                                | 1-3  | 10-500   | 1-5  |
| Enhanced terrestrial weathering                    | 0.5-4  | 50-500   | 1-5  |
| Mineral carbonation                                | –  | 50-300 ( <i>ex situ</i> ), 20 ( <i>in situ</i> ) | 3-8  |
| Ocean Alkalinity                                   | 40   | 70-200   | 2-4  |
| <b>Offshore tephra loading</b>                     | <b>0.88 <sup>a</sup></b>   | <b>~55</b>                                       | <b>2-4</b>                                     |

537

538

539